Silicon (2020) 12:101–107
https://doi.org/10.1007/s12633-019-00103-x

ORIGINAL PAPER

Alkaline Earth Based Borosilicate Glasses as Sealants in Solid Oxide Fuel Cell Applications

M. S. Salinigopal[1,2] · N. Gopakumar[2] · P. S. Anjana[1]

Received: 13 September 2018 / Accepted: 7 February 2019 / Published online: 22 February 2019

Abstract
Alkaline earth based glasses of composition $35AO - 50B_2O_3 - 15SiO_2$ (A = Ba, Ca, Sr) was prepared by conventional melt quenching technique. Density of the glasses was measured using Archimede's method. X-ray diffraction patterns confirmed the amorphous nature of the glasses. This result was supported by scanning electron microscope (SEM) image. The structure of the glasses was investigated by FT-IR spectroscopy. FT-IR spectrum revealed the characteristic bands due to various borate and silicate structural units. FT-Raman spectroscopy was used to investigate the characteristic bands of these glasses and its changes due to the presence of various alkaline earth metals. The microhardness of the glass samples was measured by indentation technique. Microhardness of all glasses were high (6.9–7.1) GPa, reflecting higher bond strength. The co-efficient of thermal expansion (CTE) were measured and lie within the range $(8–10) \times 10^{-6o}\ C^{-1}$, which was in good agreement with that of the other SOFC components.

Keywords Borosilicate glass · Density · XRD · FT-IR · Co-efficient of thermal expansion

1 Introduction

Glasses are very versatile materials because they have contributed in various fields such as electro-optic devices, thermo mechanical sensors, electronic devices, telecommunications and sealants in solid oxide fuels (SOFC) [1]. Glasses emerge as an important candidate in material science because it is easy to synthesis, relatively cheap and has the ability to control properties by varying the glass composition with chemically controlling the materials in agreement with the required applications [2, 3]. Glasses are having a specified quality of non-periodic internal arrangements which cannot be specified or differentiated by X-ray diffraction analysisas true solid [4].

In recent years, improving the mechanical property, decrease of sintering temperature and the production cost are becoming a challenge in developing new glassy materials. Modifier addition decreases the glass viscosity, increases the fraction of non-bridging oxygen containing borate and silicate structural units. Therefore, the higher amount of non-bridging oxygen decreases network connectivity and thus softening temperature and melting point [5]. Borosilicate glass is one of the choices for SOFC sealing [6].

Due to high energy efficiency, low noise, capability for internal fuel reforming, high power density and near zero emissions, solid oxide fuel cells (SOFC) have got considerable attention of researchers [7]. SOFCs have the capacity to change the production and distribution of electrical energy because of its high efficiencies and low emissions [8]. The development of a consistently good quality and robust sealant is one of the many challenges facing by researchers. Glass sealants are promising due to its low leakage rate at operating temperature. The thermal, mechanical and physical properties and viscosity of the glass sealants can be controlled by tuning the glass composition [9]. High values of microhardness of glasses reflect the higher bond strength of the glass network [10].

In the present work an attempt has been made to synthesis $35AO - 50B_2O_3 - 15SiO_2$ (A = Ba, Ca, Sr) glasses and study their physical, structural, thermal and mechanical properties.

2 Experimental Techniques

Glass samples with composition $35AO - 50B_2O_3 - 15SiO_2$ (A = Ba, Ca, Sr) were prepared with sample code as BBS,

✉ P. S. Anjana
psanjanaa@yahoo.com

[1] Department of Physics, All Saints' College, University of Kerala, Trivandrum, Kerala 695007, India

[2] Post Graduate Department of Physics, Mahatma Gandhi College, University of Kerala, Trivandrum 695004, India

CBS and SBS using conventional melt quenching technique. The glass samples were prepared by taking required stoichiometric amounts of high purity $BaCO_3$ (99.9%), B_2O_3 (99.9%), SiO_2 (99.9%), $SrCO_3$ (99.9%) and $CaCO_3$ (99.9%) all from Sigma Aldrich. The stoichiometric amounts of these oxides in mole percentage were mixed homogenously with the help of an agate mortar for 2 h and dried in an oven and then ground to fine powder. It was then melted at 1250 – 1280 °C in a Pt – crucible in a high temperature furnace. The molten glass was then poured into a pre-heated brass mould. The glass samples were immediately transferred into a pre-heated muffle furnace for annealing at 350 °C for 2 h to remove the stress due to temperature gradient, which was caused by rapid cooling. After annealing, the transparent glasses were obtained, which were polished and ground to study the density, structural, thermal and physical properties.

The prepared glass samples were subjected to X-ray diffraction (XRD) study using X-ray diffractometer (Bruker AXS D8 Advance) using CuK∞ radiation (λ = 1.5406 A°) to confirm the amorphous nature of glass samples. The density of glass samples was measured by Archimede'sprinciple using water as immersion liquid. The Fourier transform infra-red (FT-IR) spectra of the glass powder were recorded at room temperature in the region 500–1600 cm^{-1} using Shimadzu FT-IR spectrometer, Japan. FT-Raman spectra of the powdered samples were recorded in the wavenumber range 500–2000 cm^{-1} using Raman spectrometer (Alpha 3000 RA AFM & RAMAN, WITec GmbH, Ul, Germany).

Co-efficient of thermal expansion (CTE) of the glass samples were measured with a push rod dilatometer (Misura 3.32 optical flex) at a heating rate of 10 °C/min and within the temperature range 30 - 600 °C. Flat surfaces of the cylindrical pellets of thickness 6–7 mm were used for the CTE measurements. Vickers indentation technique was performed to measure the microhardness (MH) of glass samples using microhardness tester (Leica model VMHT30M). Before the measurements, the samples were diamond polished to get good reflectance surface. By trial and error method, indentation load was fixed at 50 g. Indentation was obtained by applying a 50 g load for 5 s. An average of at least 10 indentations was taken as the values of microhardness.

3 Results and Discussions

Figure 1 shows the XRD patterns of $35AO-50B_2O_3-15SiO_2$ (A = Ba, Ca, Sr) glasses. It shows two broad humps centered at 2θ ~ 30° and 45° representing two amorphous matrices, one for borate matrix and the other one related to silicate matrix which reveal the amorphous nature of glasses with the long range structural disorder [11]. This has been confirmed by scanning electron microscope (SEM) result as shown in Fig. 2. Macmillan [12] reported that thermo-physical

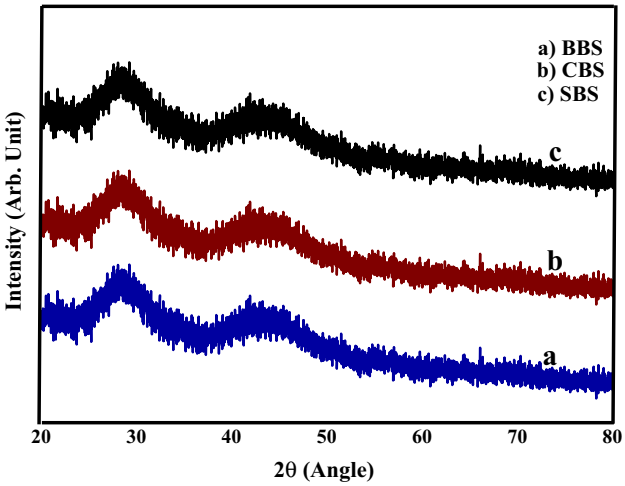

Fig. 1 XRD patterns of $35AO-50B_2O_3-15SiO_2$ (A = Ba, Ca, Sr) glasses

properties of glasses are highly dependent upon the composition. The density (ρ) and molar volume (V_m) of each glass sample is given in Table 1. The molar volume (V_m) is evaluated from density (ρ) by using the following equation:

$$V_m = \frac{M}{\rho} \tag{1}$$

Where M is molecular mass of formula unit [13].

The density of the present glasses decreases in the order of BBS, SBS and CBS respectively as shown in Table 1. The glass with BaO shows higher density (3.84 g/cm^3), which is due to the higher molecular weight of BaO (153.33 g/mol) as compared to SrO (147.63 g/mol) and CaO (100.086 g/mol) [1]. The density of glasses can be explained in terms of the relation between the mass and volume of various structural groups present in the the glass network. Hence density responds to how tightly the ions and ionic groups are packed together in the network structure [14].

Varshneya [15] reported glass as a solution. Structural changes can be related to variations in volume, so that it is

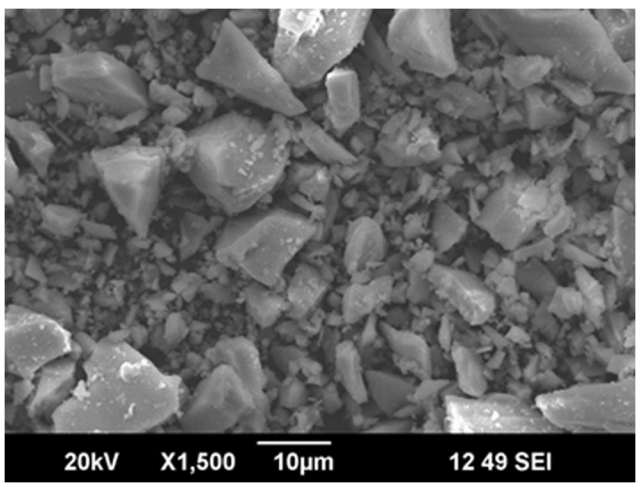

Fig. 2 Scanning Electron Micrograph of $35BaO-50B_2O_3-15SiO_2$ glass

Table 1 Variation of density, molar volume, CTE and microhardness of 35AO-50B_2O_3-15SiO_2 (A = Ba, Ca, Sr) glasses

Sample Code	Density (g/cm^3)	Molar volume	CTE (×10^{-6}°C^{-1})	Microhardness (GPa)
BBS	3.84	25.44	8.18	7.17
SBS	3.67	26.02	9.93	7.03
CBS	3.16	29.40	10.15	6.98

important to study the structural changes of the glass network in terms of molar volume rather than density. The molar volume decreases with increase in the density of the glasses, described by Eq. (1). Here V_m is higher for glass containing Ca^{2+} (29.40) and lower for glass having Ba^{2+} (25.44) (Fig. 3).

The vibrations of structural groups of atoms are not dependent on the vibrations of other atoms [16]. Figure 4 represents the FT-IR spectrum of all the glasses which reveals the characteristic bands due to various borate and silicate structural units. The FT-IR absorption bands in the borosilicate glasses are mainly observed in three regions such as 1600–1200 cm^{-1}, 1200–800 cm^{-1} and 800–600 cm^{-1} due to the asymmetric and symmetric stretching of the B – O band of triangle [BO_3] units, the B – O stretching vibration of tetrahedral [BO_4] and Si – O – Si units and the bending vibration of symmetric BO_3 units respectively [17].

The bands in the wavenumber range up to 550 cm^{-1} are attributed to the deformation vibration in Si – O groups containing SiO_4 tetrahedra [18]. In this region, the bands are observed at 524 and 541 cm^{-1} for barium borosilicate glass, at 523 cm^{-1} for strontium borosilicate and at 516 cm^{-1} for calcium borosilicate glass. Here the bands are shifted to the lower wavenumber and this change can be attributed to cation vibration (Ba^{2+} to Sr^{2+} or Ca^{2+}). In the wavenumber range of 550–650 cm^{-1}, the peak related to B –O – B bending vibration for 35AO –50B_2O_3 – 15SiO_2 is shifted from 570 cm^{-1} to 568 and 566 cm^{-1} in calcium and strontium containing borosilicate glasses respectively [19]. The bands observed in the range 650–700 cm^{-1} are

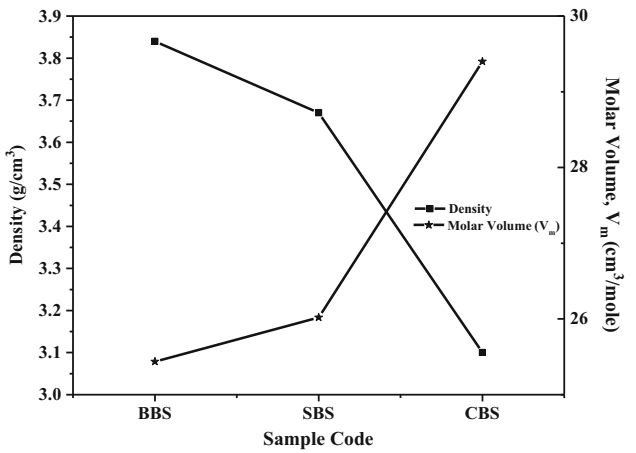

Fig. 3 Variation of density and molar volume of 35AO-50B_2O_3-15SiO_2 (A = Ba, Ca, Sr) glasses

assigned to the bending of Si – O – B linkages [20]. The peaks belonging to the stretching vibration of B – O bands in di-, tri-, tetra- and penta- borate groups consisting of BO_4 units as structural groups are in the wavenumber range 754–1198 cm^{-1}. The peaks become sharp and the intensity slightly decreases for calcium and strontium compared to barium borosilicate glasses [21, 22]. The presence of a weak band at 1539 cm^{-1}which is attributed to B – O^- stretching vibrations in BO_3 units [23], is gradually shifted to higher wavenumber. The intensity decreases considerably for calcium borosilicate and strontium borosilicate glasses. These bands are assigned to asymmetric and symmetric stretching vibration related to non-bridging oxygen atoms (NBOs) of trigonal BO_3 units in metaborate chains and rings, pyro and ortho borate groups [18].

The relative area of each component band can be calculated using the deconvoluted FT-IR spectrum. Each component band is related to some type of vibration in specific structural groups. The concentration of the structural group is proportional to the relative area of its component band [14]. The deconvolution parameters such as component band center C and relative area A of component bands can be used to calculate the fraction N_4 of BO_4 units in the borate matrix. The inset in Fig. 4. shows the deconvoluted spectrum of barium borosilicate glass. N_4, the fraction of tetrahedrally co-ordinated boron atom is defined as

$$N_4 = \frac{A_4}{A_3 + A_4} \tag{2}$$

where A_4 and A_3 represent the relative areas of BO_4 and BO_3 units. It helps to quantify the effect of alkaline earth metal ions to the relative population of BO_4 and BO_3 units [24]. To quantify the N_4 values of the glass matrix, the concentration of BO_4 units in the region 800–1100 cm^{-1} and BO_3 units the region 1100–1500 $cm^{-1}$are taken. The quantity B_4 in mol% (the form of BO_4 units) in B_2O_3 can be calculated as

$$B_4 = N_4(B_2O_3) \tag{3}$$

The component band center C (cm^{-1}) and relative area A (%) are used for calculations and the values obtained for N_4 and B_4 are tabulated in Table 2.The variation of fraction of four co-ordination boron atoms N_4 in 35AO –50B_2O_3 – 15SiO_2 (A = Ba, Ca, Sr) glasses is shown in Fig. 5.The structural changes observed in the FT-IR spectra of Ba^{2+}, Ca^{2+} and Sr^{2+} doped glass matrix evidenced by the FT-IR investigation

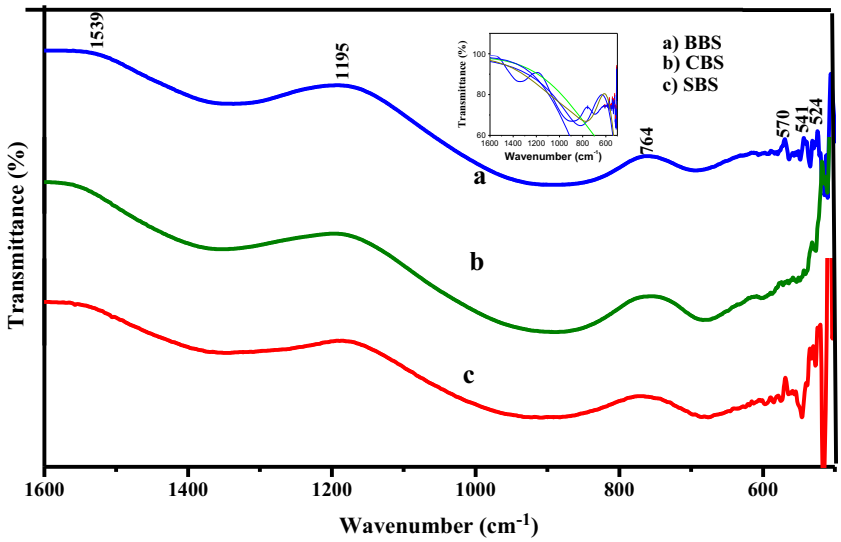

Fig. 4 FT-IR spectra of 35AO-$50B_2O_3$-$15SiO_2$ (A = Ba, Ca, Sr) glasses

suggest that the alkaline earth cations play a network modifier role in 35AO –$50B_2O_3$ – $15SiO_2$ (A = Ba, Ca, Sr) glasses.

Raman spectroscopy is a powerful tool to investigate the network structural units and bonding structure of the glass network. Raman spectra of 35AO – $50B_2O_3$ – $15SiO_2$ (A = Ba, Ca, Sr) glasses are shown in Fig. 6. Raman data can be differentiate into three regions for analysis. The first region from 400 to 850 cm^{-1} corresponds to the delocalized vibration of Si – O – Si bonding from mixed stretching and bending modes [25] and breathing vibrations of oxygen atoms in four and three member rings of BO_3 and BO_4 structural units [26, 27]. The second region from 850 to 1200 cm^{-1} includes spectral bands due to silicon Q^n vibrational modes, where Q stands for the tetrahedral symmetry of the SiO_4 unit and n is the number of bridging oxygen (BO) per Q unit to nearest silicate tetrahedral [28]. The last region lies in between 1200 and 1600 cm^{-1} due to the stretching of B – O^- bonds [O^- = Non-Bridging Oxygen (NBO)] attached to large borate (chain- and ring- type metaborate) groups [21, 29].

The band at ~ 416 cm^{-1} is assigned to the vibrations of Si – O- Si linkage (breathing, bending and rocking) [30]. The peak at ~ 487 cm^{-1} in the SBS glass system is the characteristic of

Table 2 Deconvolution parameters (component band center C (cm^{-1}) and relative area A (%)) for 35AO-$50B_2O_3$-$15SiO_2$ (A = Ba, Ca, Sr) glasses

Sample Code			N_4	B_4
BBS	C	A	0.468	23.46
	1435	3.16		
	1348	18.12		
	1238	14.14		
	1068	1.03		
	988	4.71		
	962	10.86		
	913	7.29		
	882	7.33		
CBS	1400	0.26	0.614	30.83
	1277	7.23		
	1185	2.83		
	1028	5.74		
	974	3.52		
	952	4.47		
	914	11.43		
	840	6.47		
SBS	1391	44.21	0.348	17.45
	1245	43.08		
	1121	8.82		
	1049	7.38		
	988	14.96		
	910	12.21		
	841	10.23		
	812			

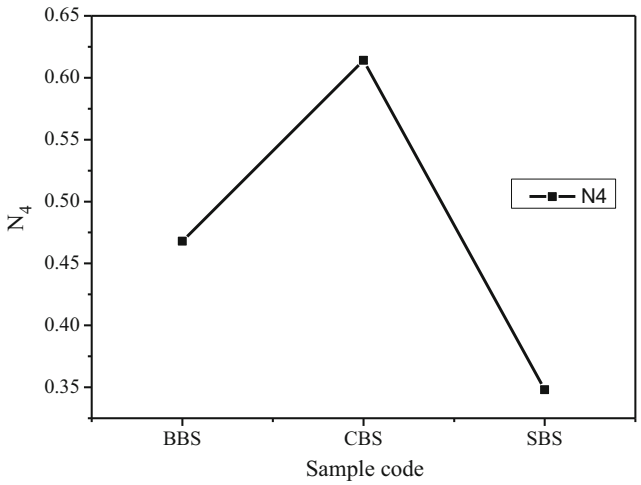

Fig. 5 Variation of fraction of four co-ordination boron atoms (N_4) of 35AO-$50B_2O_3$-$15SiO_2$ (A = Ba, Ca, Sr) glasses

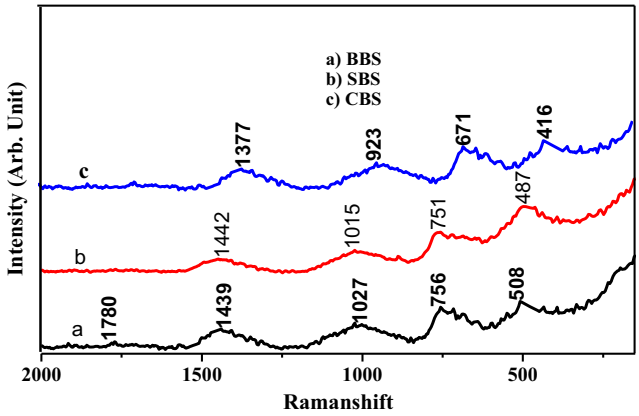

Fig. 6 FT- Raman spectra of of 35AO-50B_2O_3-15SiO_2 (A = Ba, Ca, Sr) glasses

vitreous silica. This band is assigned to the vibration of the Bridging Oxygen (BO) associated with higher membered rings of tetrahedra in the three-dimensional silicate networks [31]. The band at ~ 508 cm^{-1} appeared for BBS glass is due to the symmetric vibration of the boroxyl rings. The bands in between 750 and 790 cm^{-1} are assigned to the vibrations of six membered borate ring. Silicate structural units are mainly occurred in the second region (850–1200 cm^{-1}). The bands in this region are attributed to symmetric silicon - oxygen stretching vibrations of silicate tetrahedral units with four, three, two, one and zero NBO atoms termed as Q^0, Q^1, Q^2, Q^3 and Q^4 which belongs to isolated SiO_4^{4-} monomer, $Si_2O_7^{6-}$ dimmer, chains of SiO_3^{2-}, Si_2O_5 sheets and fully polymerized units of SiO_2 respectively [32, 33]. For CBS glass, the band having intensities at ~923 cm^{-1} is appeared due to the $Si-O^-$ symmetric stretching vibrations in Q^2 silicate structural units [34]. Raman peak observed in between 1000 and 1100 cm^{-1} are attributed to symmetric stretching vibration of SiO_4 tetrahedral units with 2 NBOs [35]. The bands occurred in the range1300–1800 cm^{-1} are caused by B – O bond stretching vibration of BO_3triagonal [36].i.e., the asymmetric stretching vibration of BO_3 triangular units in meta-borate, pyro-borate and ortho-borate groups [37]. The intensity of all bands remains almost constant for all glasses and no markable effect is detectable due to the variation of alkaline earth metal cations in the glass network. This confirms the structural stability of the present glass systems.

Microhardness of the material is an important solid-state phenomenon which is defined as the resistance offered by the material under an applied stress to the motion of dislocations deformation [38]. Microhardness of all glasses is as shown in Table 1. Microhardness increases in the order BBS (7.17 GPa), SBS (7.03 GPa) and CBS (6.98 GPa). For the present glass systems, the increase in microhardness is due to the strengthening of glass network [39]. It is clear that there is a decrease in the hardness of the present borosilicate glasses in the order of BBS,SBS and CBS respectively. This can be attributed to the low field strength of Ba^{2+} (0.26) as compared to that of Sr^{2+} (0.29) and Ca^{2+} (0.36). This variation can be linked with the structural behavior of the glass network. The change in the glass composition by alkaline earth metal ions (from Ca^{2+} to Sr^{2+} and Ba^{2+} respectively), reduces the glass resistance and forms NBO on the network formers. Microhardness and NBO in the glass network have an inverse correlation. NBO reduces the connectivity of the glass network, hence lower the microhardness of the glasses [40].

Co-efficient of thermal expansion (CTE) of the present glass systems falls in the range (8–10) × 10^{-6} $°C^{-1}$ which matches closely with that of other components of SOFC. The alkaline earth metals in the borosilicate glass network changes CTE [41]. Here the CaO (10.15) based glass has highest CTE as compared to SrO (9.93) and BaO (8.18). This is due to the strong glass network formation in CaO and SrO based glasses and hence strong bonding in the CaO and SrO based glasses compared to BaO based glass. This can be related to the field strength of the cations present in the systems ie., CTE is higher for glass having CaO which can be attributed to the highest field strength of Ca^{2+} (0.36) as compared to that of Sr^{2+} (0.29) and Ba^{2+} (0.26) [42].

4 Conclusions

Glasses with composition 35AO – 50B_2O_3 – 15SiO_2 (A = Ba, Ca, Sr) have been successfully synthesized using conventional melt quenching technique and characterized for structural and thermo-physical properties. The density of the glass samples depends on the composition of glass network. The glasses do not show major structural changes with the addition of Ba, Ca and Sr in the borosilicate glasses. Microhardness of all glasses (6.18–7.17) GPa are high which reflects the higher bond strength of alkaline earth borosilicate glasses. The CTE for all the glasses lies within the range (8–10) ×10^{-6} $°C^{-1}$, which matches with that of the other components of solid oxide fuel cell. The good structural and thermal stability and the promising physical properties show that, the present borosilicate glasses having alkaline earth metals are suitable for SOFC sealant applications.

Acknowledgements The authors would like to acknowledge SAIF, Cochin, Kerala for providing the XRD facility. The authors are also thankful to SICC, University of Kerala for the SEM image. The authors are grateful to Dr. I. Ibnusaud, IIRBS, M.G. University, Kottayam for FT-IR analysis. Authors are also thankful to SAIF, M.G. University, Kottayam for FT-Raman analysis. The authors are also thankful to Dr. Ratheesh, C-MET, Thrisur for CTE analysis.

References

1. Kaur N, Kaur G, Khan S, Singh K (2017) Conductivity, dielectric and structural studies of (30-x)SrO-xBaO-10Al_2O_3-45-SiO_2-5B_2O_3-10Y_2O_3 (5<x<25) glasses. Ionics. https://doi.org/10.1007/s11581-017-2360-y
2. Laopaiboon R, Bootjmchai C (2015) Characterization of elastic and structural properties of alkali borosilicate glasses doped with vanadium oxide using ultrasonic technique. Glas Phys Chem 4:352–358
3. Zaid MHM, Matori KA, Aziz SHA, Zakaria A, Ghazali MSM (2012) Effect of ZnO on the physical properties and optical band gap of soda lime silicate glass. Int J Mol Sci 13:7550–7558
4. Ibrahim MM, Funny MA, Hassaan MY, El-Batal HA (2016) Optical, FTIR and DC conductivity of Soda Lime Silicate Glass Containing Cement Dust and Transition Metal Ions. *Silicon* 8:443–453
5. Borhan A I, Gromada M, Nedelcu G G, Leontie L (2018) Influence of additives (CoO, CaO, B_2O_3) on thermal and dielectric properties of BaO-Al_2O_3-SiO_2 glass-ceramic sealant for OTM applications, https://arxiv.org/ftp/arxiv/papers/1507/1507.03390.pdf. Accessed 16 April 2018
6. Kothiyal GP, Goswami M, Tiwari B et al (2012) Some recent studies on glass/glass-ceramics for use as sealants with special emphasis for high temperature applications. J Adv Ceram 1:110–129.
7. Chou YS, Stevenson JW, Gow RN (2007) Novel alkaline earth silicate sealing glass for SOFC part 1. The effect of nickel oxide on the thermal and mechanical properties. J Power Sources 168: 426–433
8. Dev B, Walter ME, Arkenberg GB et al (2014) Mechanical and thermal characterization of a ceramic/glass composite seal for solid oxide fuel cells. J Power Sources 245:958–966
9. Dai Z, Pu J, Yan D, Chi B et al (2011) Thermal cycle stability of Al_2O_3-based compressive seals for planar intermediate temperature solid oxide fuel cells. Int J Hydrog Energy 36:3131–3137
10. Tiwari B, Dixit A, Kothiyal GP (2011) Study of glasses/glass-ceramics in the SrO-ZnO-SiO_2 system as high temperature sealant for SOFC applications. Int J Hydrog Energy 36:15002–15008
11. Kaur B, Singh K, Pandey OP et al (2017) Influence of modifier on dielectric and ferroelectric properties of aluminosilicate glasses. J Non-Cryst Solids 465:26–30
12. Macmillan PW (1977) Glass – ceramics. Academic press, New York, pp 1–5
13. Thombare MD (2014) Study of physical properties of Lithiumborophosphate glasses. Int J Res Pure and Appl Phys 4(2):9–15
14. Pascuta P, Pop L, Rada S et al (2008) The local structure of bismuth borate glasses doped with europium ions evidenced by FTIR spectroscopy. J Mater Sci Mater Electron 19:424–428
15. Varshneya AK (1994) Density and molar volume, fundamentals of inorganic glasses. Academic press, New York
16. Rejisha SR, Anjana PS, Gopakumar N (2016) Effect of cerium (IV) oxide on the optical and dielectric properties of strontium bismuth borate glasses. J Mater Sci Mater Electron 27:5475–5482
17. Mandal AK, Agrawal D, Sen R (2013) Preparation of homogeneous barium borosilicate glass using microwave energy. J Non-Cryst Solids 371:41–46
18. El-Egili K (2003) Infra-red studies of Na_2O – B_2O_3 – SiO_2 and Al_2O_3 – Na_2O – B_2O_3 – SiO_2 glasses. Physica B 325:340–348
19. Abo-Naf SM, El-Sayed MK, El-Sayed E-SM et al (2015) In vitro bioactivity evaluation, mechanical properties andmicrostructural characterization of Na_2O–CaO–B_2O_3–P_2O_5 glasses. Spectrochim Acta A Mol Biomol Spectrosc 144:88–98
20. Elbatal FHA, Khalil MMI, Nada N, Desouky SA (2003) Gamma rays interaction with ternary silicate glasses containing mixed CoO + NiO. Mater Chem Phys 82:375–387
21. Kamitsos EI, Karakassides MA, Chryssikos GD (1987) Vibrational spectra of magnesium – sodium – borate glasses.2.Raman and mid – infrared investigation of the network structure. J Phys Chem 91:1073
22. Kamitsos EI, Karakassides MA, Chryssikos GD (1987) A vibrational study of li-borate glasses with high LiO_2 content. Phys Chem Glasses 28:203–209
23. Kaur R, Singh S, Pandey OP (2012) FTIR structural investigation of gamma irradiated BaO-Na_2O-B_2O_3-SiO_2 glasses. Physica B 407:4765–4769
24. Rejisha SR, Santha N (2011) Structural investigations on 20MO-xBi_2O_3-(80-x)B_2O_3 (M=ca, Sr and Ba; x=15and 55) glasses. J Non-Cryst Solids 357:3813–3821
25. Kamitsos EI, Kapoutsis JA, Jain H, Hsieh CH (1994) Vibrational study of the role of trivalent ions in sodium trisilicateglass. J Non-Cryst Solids 171:31–45
26. Furukawa T, Whtte WB (1981) Raman spectroscopic investigation of sodium borosilicate glass structure. J Mater Sci 16:2689–2700
27. Eremyashev VE, Osipov AA, Osipova LM (2011) Borosilicate glass structure with rare-earth-metal cations substituted for sodium cations. Glas Ceram 68(7–8):205–208
28. Gaskell PH (1991) In: Zarzcycki J (ed) Materials science and technology, glasses and amorphous materials, Vol 9. Wiley -VCH, Weinheim
29. Chryssikos GD, Kamitsos EI, Patsis AP, Bitsis MS, Karakassides MA (1990) Thedevitrification of lithium metaborate: polymorphism and glass formation. J Non-Cryst Solids 6:42–51
30. Gavenda T, Gedeon O, Jurek K (2017) Structural and volume changes and their correlation in electron irradiated alkali silicate glasses. Nucl Inst Methods Phys Res. B 397:15–26
31. Kacema IB, Gautron L, Coillot D, Neuville DR (2017) Structure and properties of lead silicate glasses and melts. Chem Geol 461: 104–114
32. McMillan P (1984) Structural studies of silicate glasses and melts applications and limitations of Raman spectroscopy. Am Mineral 69:622–644
33. Matson DW, Sharma SK, Philpotts JA (1983) The structure of high silica alkali-silicate glasses. A Raman spectroscopic investigation. J Non-Cryst Solids 58:323–352
34. Rezazadeh L, Baghshahi S, NozadGolikand A, Hamnabard Z (2017) Structure, phase formation, and wetting behaviour of BaO–SiO_2– B_2O_3 based glass–ceramics as sealants for solid oxide fuel cells. Ionics 20:55–64. https://doi.org/10.1007/s11581-013-0934-x
35. Berwal N, Dhankhar S, Sharma P, Kundu RS, Punia R, Kishore N (2017) Physical, structural and optical characterization of silicate modified bismuth-borate-tellurite glasses. J Mol Struct 1127:636–644
36. Kaky KM, Lakshminarayana G, Baki SO, Lira A, Meza-Rocha AN, Falcony C, Caldino U, Kityk IV, Taufiq-Yap YH, Halimah MK, Mahdi MA (2017) Structural and optical studies of Er^{3+} doped alkali/alkaline oxide containing zinc boro-aluminosilicate glasses for 1.5 mm optical amplifier applications. Opt Mater 69:401–419
37. Nanda K, Berwal N, Kundu RS, Punia R, Kishore N (2015) Effect of doping of Nd3+ ions in BaO–TeO2–B2O3 glasses: A vibrational and optical study. J Mol Struct 1088:147–154
38. Patil AL (2017) Measurments of Vickers hardness and refractive index properties of Na- Borophosphate glasses. Int J ChemTech Res 10(12):138–142

39. Zhang Q, Du X et al Effect of Nb_2O_5 doping on improving the thermo-mechanical stability of sealing interfaces for solid oxide fuel cells. Sci Report 7(5355). https://doi.org/10.1038/s41598_017_05725_y
40. Barlet M, Delaye JM, Charpentier T, Gennisson M, Bonamy D, Rouxel T, Rountree CL (2015) Hardness and toughness of sodium borosilicate glasses via Vickers's indentations. J Non-Cryst Solids 417–418:66–79
41. Meinhardt KD, Kim DS, Chou YS et al (2008) Synthesis and properties of a barium aluminosilicate solid oxide fuel cell glass–ceramic sealant. J Power Sources 182:188–196
42. Kumar V, Arora A, Pandey OP et al (2008) Studies on thermal and structural properties of glasses as sealants for solid oxide fuel cells. Int J Hydrog Energy 33:434–438